T3E3 Report: Solid State Spins

6.2410 Quantum Engineering Platforms
Daniel Sanango

I. Introduction

In this station, we investigate the strong coupling effects between nitrogen-vacancy (NV) centers in diamonds and a microwave resonator. We begin by simulating the expected strong coupling behavior to refine experimental parameters and optimize system performance. Building on these simulations, we aim to achieve strong coupling experimentally to demonstrate coherent energy exchange between the NV centers and the resonator.

II. Week 1 Summary

The objective of this lab exercise was to characterize our given microwave cavity and Helmholtz coil. The Helmholtz coil applies a magnetic field to a dielectric cavity housing a diamond. The diamond is specially prepared with a nitrogen-vacancy (NV) setup. The setup allows an easily-manipulatable spin state that responds strongly to certain frequencies and surrounding magnetic fields. The magnetic field tunes the NV spin magnetic frequency, varying the resonant frequency of the system. To measure the reflection coefficient response to frequency changes in the system, we attached a metal loop of variable length to a VNA. The VNA allowed us to sweep ranges of frequencies.

First, we measured the given cavity's resonance frequency. Given the following formulas and parameters pertaining to the setup:

$$\zeta tan(\frac{\zeta L}{2}) = \zeta_0 \tag{1}$$

$$\zeta = \sqrt{\epsilon_r \frac{\omega_c^2}{c^2} - \frac{x_{01}^2}{r_d^2}} \tag{2}$$

$$\zeta_0 = \sqrt{\frac{x_{01}^2}{r_d^2} - \frac{\omega_c^2}{c^2}} \tag{3}$$

$\epsilon_r = 73$ (relative permittivity of cavity dielectric)
$r_d = \frac{17.5}{2} \cdot 10^{-3}[m]$ (radius of cavity dielectric)
$x_{01} = 2.4048$ (zero of Bessel function)
$L = 6.62 \cdot 10^{-3}[m]$ (dielectric height)

Solving this system, we find that $\omega_c = 1.30 \cdot 10^{10}[rad/s]$, giving $f_c = \frac{1.30}{2\pi} \cdot 10^{10}[Hz] = 2.07[GHz]$

We then experimentally obtained the resonant frequency of the setup using a VNA and a metal loop above the cavity. To do this, we looked for a strong dip on the VNA's S_{21} sweep and noted the frequency location of occurrence. We then adjusted the metal loop to vary the bandwidth of our measured S_{21} value. We sought to obtain an S_{21} dip with a small bandwidth and steep dip. These parameters give the strongest frequency response, thus making them ideal parameters. After optimizing the height of the loop, we found that $\omega_c = 1.11 \cdot 10^{10}[rad/s]$, giving $f_c = 1.77[GHz]$

After this, we used a Gauss meter to characterize the Helmholtz coil, measuring the output magnetic field based on voltage variation from a power supply. Figure 1 demonstrates a linear relation between the parameters, which is expected. NOTE: Earth's magnetic field generates 0.6[G], which is present in our measurement.

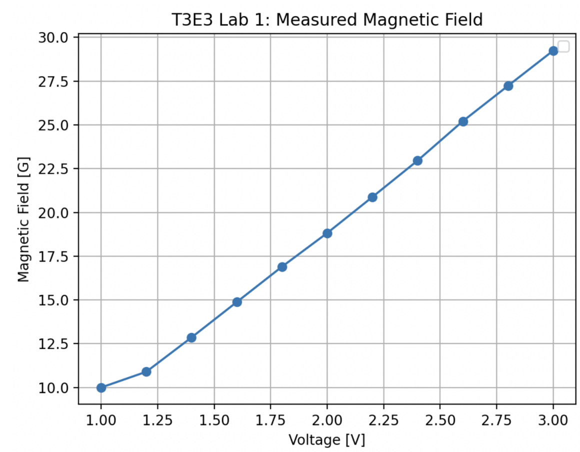

Fig. 1: Measured magnetic field [G] vs applied Voltage [V] for Helmholtz Coil Setup

Noting this relationship, we determined that the number of loops per coil on the Helmholtz coils was approximately 2014.6.

We are given the fomula:

$$\Gamma(\omega) = -1 + \frac{\kappa_{c1}}{\frac{\kappa_c}{2} + j(\omega - \omega_c) + \frac{g^2}{\frac{\kappa_s}{2} + j(\omega - \omega_s) + \alpha}} \tag{4}$$

We are also given the following parameters:
$g = 0$ (ignoring coupling effects, will account for later)
$\alpha = 0$
$\kappa_s = \frac{2}{T_2} = \frac{2}{20 \cdot 10^{-6}}[Hz]$

After this, we measured the cavity's intrinsic Q by noting its response to the variation in the loop's height from the cavity. Measuring the quality factor variations, we were able to produce Figure 2. From this, we determined that $Q_0 = 14961$, giving $\kappa_c = \frac{\omega_c}{14961}$. Given the best-fit plot result from Figure 2, we also determined that the figure's leading coefficient (19062) gave insight to the value of $\kappa_{c1} = \omega_c(\frac{1}{14961} - \frac{1}{19602})$

Ultimately, with this information, we produced Figures 3, 4, 5, and 6.

Accounting for the system's coupling effects, we now set $g = 1.01 \cdot 10^{-6}$ and ran the same analyses as with $g = 0$. This generated Figures 7, 8, 9, and 10.

Based on the reflection coefficient formula, we expect the coupling to introduce a "disturbance" in the $g = 0$ case with a sloped line intersecting $\omega = \omega_s$ and our estimated range of frequencies for the resonant point. As we vary the magnetic field, we also expect the resonant point to shift, which is demonstrated in the figures.

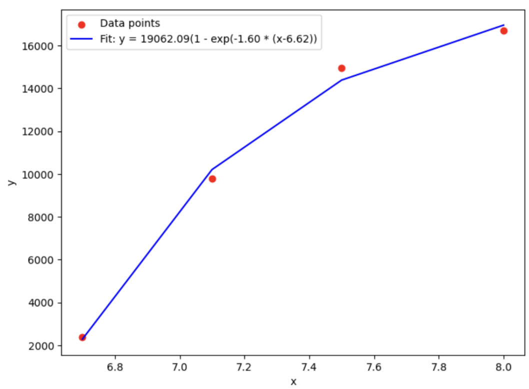

Fig. 2: Quality Factor vs Coupler Height [cm]

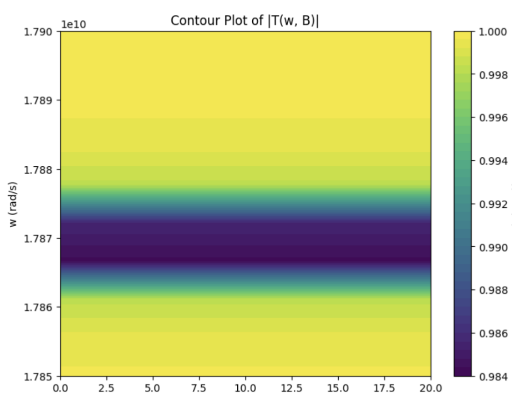

Fig. 3: $g = 0$, Magnitude of Reflection Coefficient vs Frequency and Magnetic Field

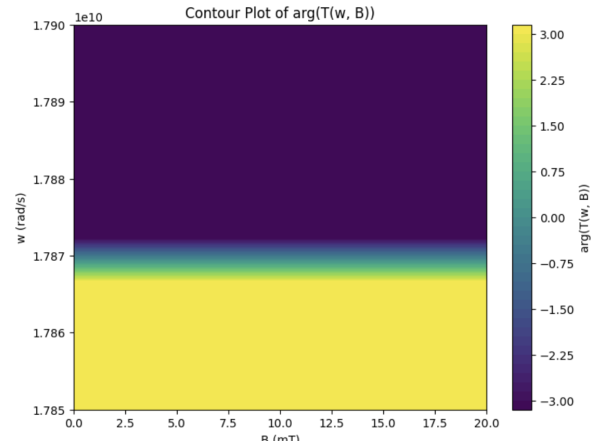

Fig. 4: $g = 0$, Argument of Reflection Coefficient vs Frequency and Magnetic Field

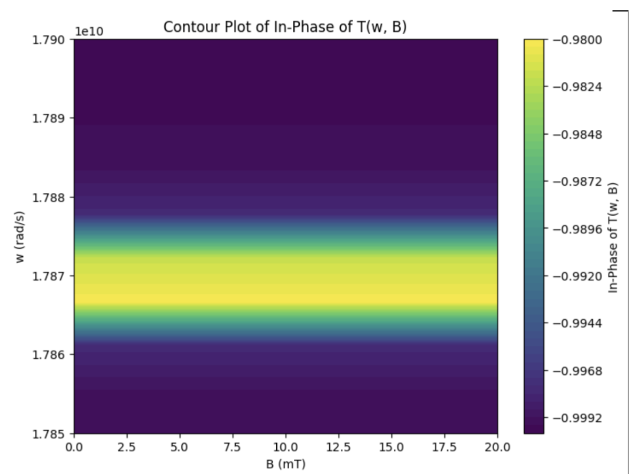

Fig. 5: $g = 0$, In-Phase of Reflection Coefficient vs Frequency and Magnetic Field

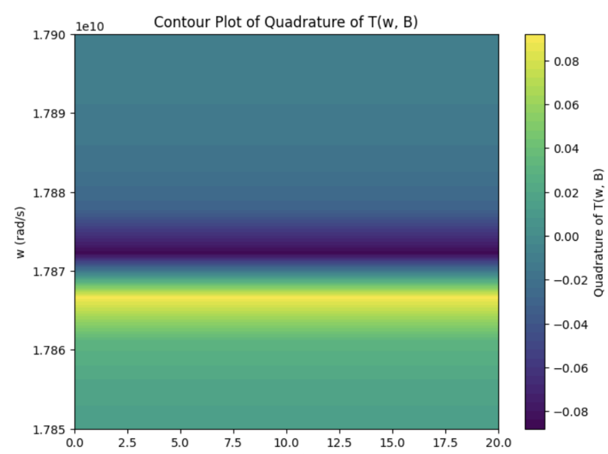

Fig. 6: $g = 0$, Quadrature of Reflection Coefficient vs Frequency and Magnetic Field

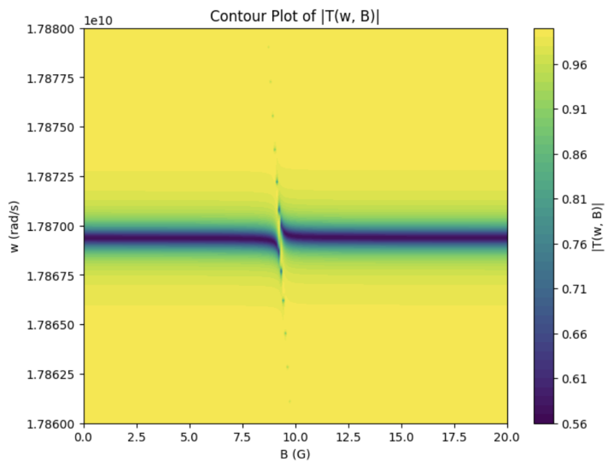

Fig. 7: $g \neq 0$, Magnitude of Reflection Coefficient vs Frequency and Magnetic Field

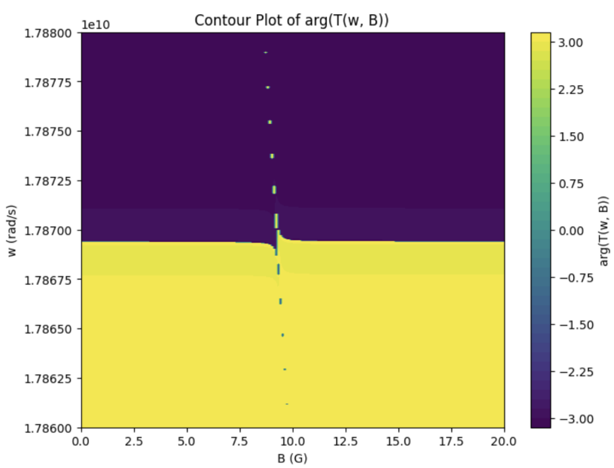

Fig. 8: $g \neq 0$, Argument of Reflection Coefficient vs Frequency and Magnetic Field

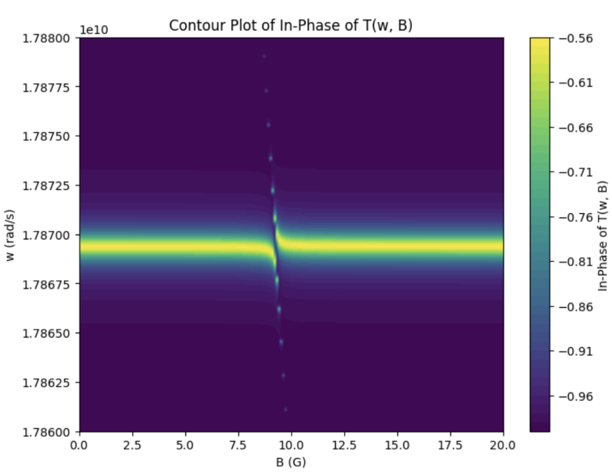

Fig. 9: $g \neq 0$, In-Phase of Reflection Coefficient vs Frequency and Magnetic Field

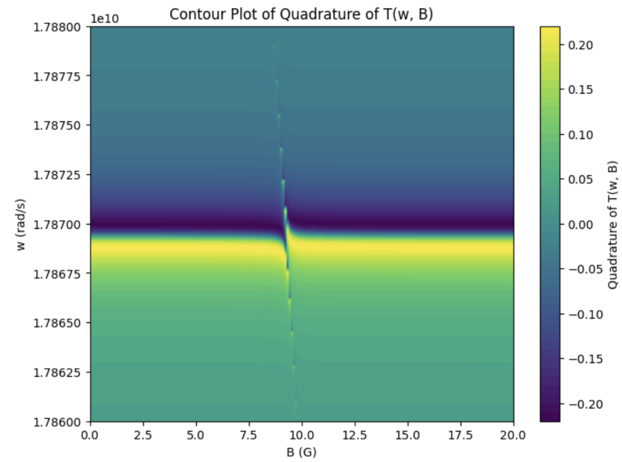

Fig. 10: $g \neq 0$, Quadrature of Reflection Coefficient vs Frequency and Magnetic Field

III. Week 2 Summary

This objective of this week was examine the resonant frequency shift with an applied magnetic field. In doing this, we would be able to assess the magnetic field sensitivity of our setup.

In this exercise, we used a class IV laser to achieve strong coupling between the NV centers and microwave resonator. A class IV laser's power output was necessary to clearly see a change in the resonant frequency. We also used a mechanical iris to limit light from entering or exiting the system. This ensured ambient light would not mess up our experiment. It also ensured high-power laser light did not exit the system.

We used Python interfaces with our VNA and power supply to set system parameters and acquire data. To ensure the applied magnetic field made a viewable change on our system, we narrowed the frequency range to about our previously-identified resonance frequency point. To ensure our data was accurate, we took numerous sweeps and averaged our measured argument and magnitude values. We also computed the variance of our data. Figure 11 demonstrates our findings. There is a clear "bend" in the data around 4-10[G], demonstrating the magnetic field's effect on the system's resonant frequency. This is consistent with our logic from week 1.

Observing the diamond with the laser at a low power output, we observed a slight fluorescence in the diamond. From Figure 12, placing a 638[nm] optical longpass filter in front of the diamond would still permit most fluorescence to pass.

After obtaining this data, we can now determine the system's maximal magnetic field sensitivity. Using the formula:

$$V_{rms} = \sqrt{P_{in} \cdot R} \tag{5}$$

Where,...
P_{in} = power from VNA
$R = 50[\Omega]$, impedance of VNA

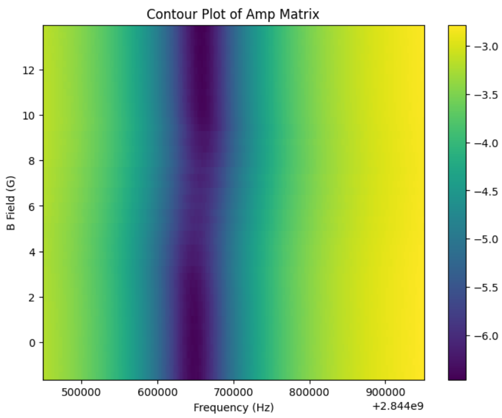

Fig. 11: Argument of Reflection Coefficient vs Frequency and Magnetic Field

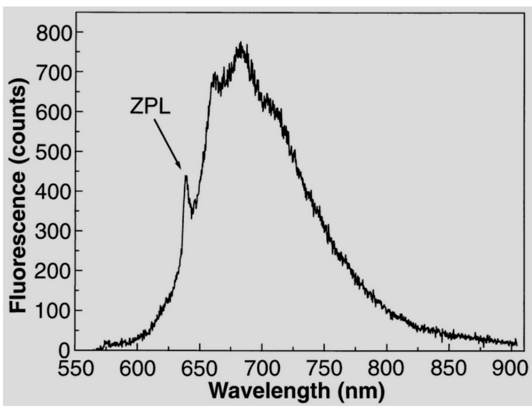

Fig. 12: Fluorescence of Diamond [6.2410 Github]

From the nanoVNA, it is known that $P_{in} = -10[dBm] = 10^{-1}[mW]$. We are also given that the phase noise is $-103\frac{dBc}{Hz} = 10log_{10}(x)$. Manipulating this relation, we get:

$d\phi = \sqrt{10^{-130/10}} = 10^{-5}[\sqrt{Hz}]^{-1}$

Therefore,...

$\frac{V_{rms}}{\sqrt{Hz}} = 7.07 \cdot 10^{-7}[\frac{V}{\sqrt{Hz}}]$

Using these procedures, we can now make a 2D plot of $\frac{dV}{dB}$ vs B and V. This result is demonstrated in Figure 13.

From the graph, we find that the maximum $\frac{dV}{dB}$ value is 0.0012. We can now compute the maximum magnetic field intensity:

$$\frac{d\phi}{(\frac{dV}{dB})_{max}} = \frac{7.07 \cdot 10^{-7}}{0.0012 \cdot 10^{4}} = 5982[\frac{pT}{\sqrt{Hz}}] \quad (6)$$

IV. Conclusion

In conclusion, we successfully demonstrated the sensitive nature of NV diamonds in an external magnetic field. By applying a magnetic field to our cavity setup, we saw a clear shift in the resonant frequency of the system. We also simulated the effects of our setup on a digital twin to understand what we expected to see and the math that supported it.

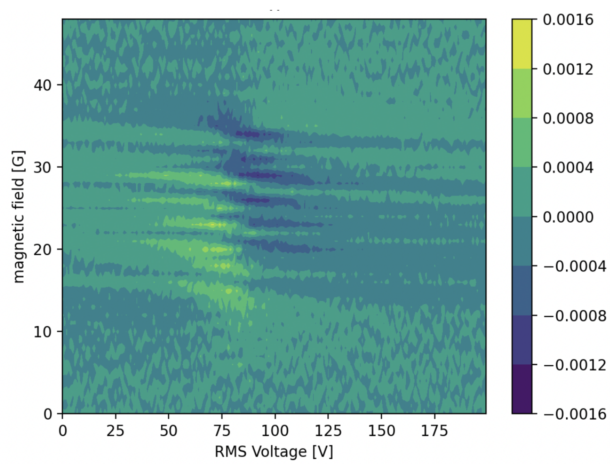

Fig. 13: Fluorescence of Diamond [6.2410 Github]

Uses for these procedures include ultra-precise magnetic field trackers. A NV diamond's ability to react to extremely small changes in magnetic fields can be used to analyze minuscule changes in fields, like the magnetic behavior of brain waves. It can also be used to characterize magnetic hotspots throughout the world, making a non-satellite GPS system possible.